

# A thermo-mechanical interface model for simulating the bond behaviour of FRP strips glued to concrete substrates exposed to elevated temperature



Antonio Caggiano<sup>a,\*</sup>, Diego Said Schicchi<sup>b</sup>

<sup>a</sup> CONICET (Argentina's Natl. Council of Scientific and Technical Research) and University of Buenos Aires, Argentina

<sup>b</sup> Stiftung Institut für Werkstofftechnik (IWT), 28359 Bremen, Germany

## ARTICLE INFO

### Article history:

Received 15 May 2014

Revised 6 October 2014

Accepted 8 October 2014

### Keywords:

Debonding

Fiber/matrix bond

High-temperature properties

Thermomechanics

Interface

## ABSTRACT

This paper proposes a model aimed at simulating the bond behaviour of Fiber Reinforced Polymer (FRP) laminates glued to concrete substrates and exposed to high temperature. Based on a previous model already formulated by one of the authors and available in the scientific literature, the present paper proposes a theoretical model formulated within the general framework of Fracture Mechanics and Plasticity-based concepts. Particularly, the aforementioned model is extended herein to consider the thermal effects, through a temperature-based scaling function affecting the strength parameters and softening rules which define the failure surface and the post-cracking response of FRP-concrete joints. The mechanical soundness of the proposed model is demonstrated by the very good agreement between some experimental results taken from the scientific literature on FRP-to-concrete systems tested in pull-out loading at normal and elevated temperature and the corresponding theoretical simulations.

© 2014 Elsevier Ltd. All rights reserved.

## 1. Introduction

The use of composite materials is one of the most recent advances in strengthening existing structures made of either concrete [1,2] or masonry [3,4]. Particularly, techniques based upon utilising Externally Bonded (EB) Fiber Reinforced Polymer (FRP) strips is one of the most common practices for structural strengthening [5]. Adhesive connection is by far the most common solution to connect FRP laminates to the above mentioned materials, even though an innovative anchorage technique for prestressed Carbon-Fiber Reinforced Polymer strips has recently been proposed [6]. Moreover, the use of FRP strips also gained its popularity, not only for repairing cement-based or masonry buildings, but also for upgrading steel structures or wood frames [7].

Several investigations currently available in the scientific literature point out the importance of the bond between composite strip and concrete substrate as a controlling factor in designing structural strengthening interventions [8]. Actually, different test set-ups have been proposed for investigating the bond behaviour of FRP strips glued to concrete or masonry substrates. They are often classified as follows: single and double pull-out schemes,

single debonding with fixed back side, critical diagonal crack induced interfacial debonding or intermediate crack-induced debonding [9].

Both experimental [10,11] and theoretical [12,13] researches are currently available in the scientific literature for investigating the bond-slip behaviour of FRP-to-concrete interface under quasi-static and monotonic load conditions. However, the influence of critical conditions like high temperature and fire on the overall performance of such a structures still represents an open topic which needs to be further investigated. As a matter of fact, both matrix and bond adhesive are thermosetting polymers (epoxies) characterised by a very low glass transition temperature  $T_g$  [14,15]. This implies that the actual mechanical properties of FRP plates and sheets are strongly affected by the exposure to high temperatures, that directly modifies the FRP-adhesive and adhesive-concrete interfaces, especially when such temperatures achieve the  $T_g$  value [16–18]. It is worth highlighting that a higher  $T_g$  temperature typically characterises the FRP matrix compared with the  $T_g$  of the adhesive epoxy employed for the FRP-to-concrete joint. This implies that, under elevated temperatures, the weak link of a FRP-to-concrete bonded joint is represented by the epoxy adhesive.

In some cases the Young's modulus  $E_f$  of the FRP laminate is highly sensitive to temperature changes. Available test data on FRP sheets [19,20] and FRP bars [21,22] at elevated temperatures

\* Corresponding author.

E-mail addresses: [acaggiano@fi.uba.ar](mailto:acaggiano@fi.uba.ar) (A. Caggiano), [schicchi@iwt.uni-bremen.de](mailto:schicchi@iwt.uni-bremen.de) (D. Said Schicchi).

## Nomenclature

$s$	relative joint slip	$T_{avg,0}$	input temperature parameter
$s^e$	elastic part of the relative joint slip	$T_{avg,f}$	input temperature parameter
$s^p$	plastic part of the relative joint slip	$T_g$	glass transition temperature
$\bar{s}^T$	thermal part of the relative joint slip	$\zeta_\tau$	decay function describing the shape of the stiffness degradation against thermal processes
$\tau$	interface shear stress	$H$	softening parameter related to mechanical actions
$d_T$	thermal damage variable	$I$	softening parameter related to temperature
$k_E$	undamaged tangential elastic stiffness	$k_d^{ep}$	tangential interface stiffness
$k_{E,d}$	tangential elastic stiffness	$\vartheta$	thermal tangential stress
$\Delta T$	interface temperature jump	$q_n$	convective law
$\alpha_s^0$	coefficient of the thermal (surface) expansion	$h_f$	convective heat transfer coefficient
$\lambda$	non-negative plastic multiplier	$u^+$	normal (positive) interface separation
$f$	failure criterion	$h_0$	maximum convective coefficient related to a closed crack
$\tau_y$	interface shear strength	$h_{inf}$	minimum convective coefficient related to a fully opened crack
$\tau_{y,0}$	initial (maximum) shear strength	$l_f$	bonding length
$\psi$	scaling function	$b_f$	plate width
$w_{st}$	work spent in mode II	$t_f$	plate thickness
$G_f$	fracture energy in mode II	$E_f$	effective young's modulus of the plate
$\xi$	ratio between work spent and fracture energy	$F$	pull-out load
$\alpha$	scalar function controlling the shape of the softening rule		
$\eta$	temperature-based rule		
$\theta$	scalar variable describing the thermal damage		
$T_{avg}$	average temperature in the interface plane		

actually demonstrate as the elastic properties of such FRPs predominantly depend on the glass transition temperature of the polymer matrix  $T_g$ .

In this regard, simple empirical models are available in literature to describe the elastic modulus degradation of FRP under elevated temperature [23,24]. Studies performed on adhesive materials exposed to temperature close to  $T_g$  clearly highlight the strong reduction of their mechanical properties in terms of tensile strength, elastic modulus and bond properties [25]. Moreover, depending on the type of resin used by FRP manufacturers, the value of  $T_g$  may range between 70 °C and 175 °C [26]. Even though this range can be taken as a reference for prefabricated FRP products, for FRP sheets glued with epoxy materials  $T_g$  is around 45–82 °C [27]. Therefore, based on this knowledge, in this work the expression “elevated temperature” is intended to be referred to temperatures rather close or even higher than  $T_g$  limit.

Only few experimental works, available in the scientific literature, investigate the mechanical response of FRP-concrete interface at elevated temperature. In this field, an interesting research by Tadeu and Branco [28] reports the effect of high temperature on the bond between EB steel reinforcement and concrete supports. The results of this work highlight that the epoxy resin, representing the bonding material between steel reinforcement and concrete elements, actually exhibited a very poor behaviour when subjected to increased temperature. Double pull-out shear tests on concrete elements, reinforced with EB Carbon-FRP [29–31] and Glass-FRP laminates [32] at different temperatures represent interesting works on this subject. The experimental study by Blontrock et al. [29] on CFRP-to-concrete bonded joints considered four different temperatures (i.e., 20, 40, 55 and 70 °C). The overall pull-out strength in those tests increased 41% and 24% when the temperature raised from 20 °C to 40 °C and 55 °C, respectively. However, when the temperature was further increased up to 70 °C (near to the  $T_g$  temperature), the ultimate load decreased 19%. Moreover, Klamer et al. [30] stated that two types of failure can be observed based on the considered temperature. For low to moderate temperatures (up to 40 °C) failure occurred in the concrete layer, while for elevated temperatures (50–75 °C) failure

occurred at the adhesive-concrete interface without leaving any concrete attached to the adhesive. The experimental results by Wu et al. [31] highlighted that the value of the measured fracture energy decreases while the effective bonding length increases at temperatures near to or higher than  $T_g$ . Elevated temperature (especially when the  $T_g$  is reached) significantly affects the bond between FRP and concrete interfaces dealing with a sensible reduction of the pull-out strength as demonstrated in [32]. The influence of temperature on bonded FRP-to-concrete joint systems tested under three-point bending schemes is also presented in the work of Di Tommaso et al. [33]: the experimental campaign points out as the failure mode mainly changes with temperature. Particularly, a more ductile response was registered at high temperatures while brittle failures occurred at low and negative temperatures.

Various national and international codes and guidelines aim at designing FRP-strengthened RC structures [27,34,35]. Such codes mainly cover applications in which temperature effects are not relevant. As a matter of fact, there are no specific standards dealing with FRP-concrete structures under high temperature: the existing ones, e.g. the ACI440-2R-08 [27] guideline, directly suggests that, in case of fire, the possible contribution of FRP to the load-carrying capacity of strengthened members should be neglected.

However, several theoretical models are currently available to simulate the debonding failure of FRP strips glued to brittle substrates. The most common ones are based on assuming that the fracture process propagates in pure “mode II” and consider bond-slip laws which describe the interface behaviour and can be taken as a bilinear elastic-softening relationship [1], a hyperbolic law [36] or a rational bond-slip law [37]. All available formulations for describing the FRP-to-concrete bond-slip behaviour generally do not take into account damage effects induced by thermal conditions. In fact, only few contributions are available in scientific literature: e.g., the 3D model by Gamage et al. [38] capable to predict the heat transfer response of CFRP strengthened concrete members as well as the recent proposal by Dai et al. [24] outlining a nonlinear bond-slip model for FRP laminates externally bonded to concrete under elevated temperature.

Therefore, this work is intended at giving a contribution in this field, by proposing a coupled thermo-mechanical fracture-based model to simulate the degradation effect of high temperature on the bond between FRP and concrete. The formulation is implemented into zero-thickness interface elements for discontinuous finite element analyses and is formulated within the general framework of Fracture Mechanics, according to the well-known discontinuous crack model. The fracture propagation and the corresponding stress release process is simulated through a general nonlinear temperature-based softening relationship, though assuming that fracture develops in “mode II”.

After this general introduction about the State-of-the-Art and main motivations of this research, it is worth highlighting that the paper is organised as follows. Section 2 deals with the basic assumptions of the finite element analysis to simulate the bond behaviour under pull-out test of FRP plates glued on a concrete substrate. Section 3 reports the general formulation of the elasto-thermo-plastic model featuring fracture energy-based softening and thermal damage being this latter the key novelty contribution of this paper. Then, Section 4 figures out the heat transfer problem along the interface element and, finally, Section 5 proposes the model validation and reports some comparisons between a series of experimental results, available in the scientific literature and often assumed as a benchmark, and the corresponding numerical simulations.

## 2. Bond behaviour of FRP-to-concrete joint exposed to high temperature: Fundamental assumptions

The main assumptions for the Finite Element (FE) simulation of bond-slip behaviour of FRP laminates glued to a concrete substrate (Fig. 1) exposed to elevated temperature are presented below:

1. FRP strips are modelled as a thermo-elastic material through one-dimensional two-nodes isoparametric trusses.
2. The adhesive layer between FRP laminate and concrete substrate is simulated through an elasto-thermo-plastic constitutive relationship for interface elements. Such a constitutive model, considered for modelling the nonlinear response of FRP-to-concrete joints, is formulated within the general framework of Fracture Mechanics combined with thermal effects inducing softening degradations. All thermal and mechanical nonlinearities are lumped at the interface between the FRP laminate and the concrete substrate.
3. The temperature field is characterised by a discontinuity across the interface due to strong discontinuities of the interface kinematics.
4. The heat flow, normal to the interface plane, is kept constant since no strong kinematic (normal discontinuity) was considered.
5. The concrete substrate is ideally considered as a rigid block: thus, strains developed in concrete are neglected.

## 3. Coupled fracture energy-based thermal interface model

This section presents the key aspects of the interface model proposed for simulating the fracture process at the FRP-concrete substrate exposed to elevated temperature. As classically assumed in the Flow Theory of Plasticity, constitutive equations can be written in the so-called incremental formulation

$$\begin{aligned}\dot{s} &= \dot{s}^e + \dot{s}^p + \dot{s}^T \\ \dot{\tau} &= k_{E,d} \dot{s}^e \\ \dot{\tau} &= k_{E,d} (\dot{s} - \dot{s}^p - \dot{s}^T)\end{aligned}\quad (1)$$

where  $\dot{s}$  is the rate of the relative joint slip, decomposed into elastic, plastic and thermal components,  $\dot{s}^e$ ,  $\dot{s}^p$  and  $\dot{s}^T$ , respectively;  $\dot{\tau}$  is the rate of interface shear stress and  $k_{E,d}$  defines the tangential elastic stiffness, thermally degraded through the damage (scalar) variable,  $d_T$ ,

$$k_{E,d} = d_T k_E \quad (2)$$

being  $k_E$  the elastic undamaged stiffness.

Beside the classical assumptions usually adopted for interface approaches which consider a jump in the displacement field (kinematic discontinuity) and the continuity of the stress field, the present proposal assumes that the temperature field develops a jump across the FRP-to-concrete interface, mainly due to strong discontinuities of the interface kinematics [39].

The norm of the temperature jump is calculated as  $[\|\Delta T\|] = [|T^+ - T^-|]$ , being  $T^+$  and  $T^-$  the temperature at the “+” and “-” side of the considered interface. The rate of the relative joint slip due to thermal effects,  $\dot{s}^T$ , is assumed to be isotropically linear to the rate of the temperature jumps  $\Delta \dot{T}$  [39]

$$\dot{s}^T = \alpha_s^0 [|\Delta \dot{T}|] \quad (3)$$

where  $\alpha_s^0$  is a coefficient of the thermal (surface) expansion.

Then, according to the classical flow rule of plasticity, the inelastic slip rate can be defined as

$$\dot{s}^p = \dot{\lambda} \frac{\partial f}{\partial \tau} \quad (4)$$

where  $\dot{\lambda}$  is the non-negative plastic multiplier derived by means of the classical Kuhn–Tucker and consistency conditions which take the following expressions

$$\dot{\lambda} \geq 0, \quad f \leq 0, \quad \dot{\lambda} f = 0, \quad \dot{f} = 0 \quad (5)$$

where  $f = f(\tau, \tau_y)$  describes the elastic criterion in post-peak regime

$$f(\tau, \tau_y) = \tau^2 - \tau_y^2 \leq 0 \quad (6)$$

depending on both the current shear stress  $\tau$  and the evolution of the yielding one-dimensional surface  $\tau_y$ .

The variation in  $\tau_y$  is assumed to depend on the combined effects of both the spent fracture work and the agent temperature. The following relationship is proposed

$$\tau_y = \tau_{y,0} (1 - \psi)(1 - \eta) \quad (7)$$

in which  $\tau_{y,0}$  is the maximum shear strength, which represents a material parameter of the model,  $\psi$  the scaling function defined by Carol et al. [40], while  $\eta$  is the proposed temperature-based rule which actually quantifies the damage induced by thermal effects.

### 3.1. Fracture-energy softening evolution

The  $\psi$  function of Eq. (7) is given as follows

$$\psi(\xi) = \frac{e^{-\alpha \xi}}{1 + (e^{-\alpha} - 1)\xi} \quad (8)$$

being  $\xi = w_{sl}/G_f$ , the ratio between the inelastic work spent,  $w_{sl}$ , with the available fracture energy in Mode II,  $G_f$ ; the softening parameter  $\alpha$  of Eq. (8) provides a series of descending softening curves as described in Caggiano and Martinelli [41].

The incremental fracture work  $\dot{w}_{sl}$  in debonding is defined as

$$\dot{w}_{sl} = \tau \dot{s}^p. \quad (9)$$

It follows that the total dissipated work is obtained by integrating the fracture work increments during the delamination process. The variable  $w_{sl}$  defines the amount of plastic work which leads

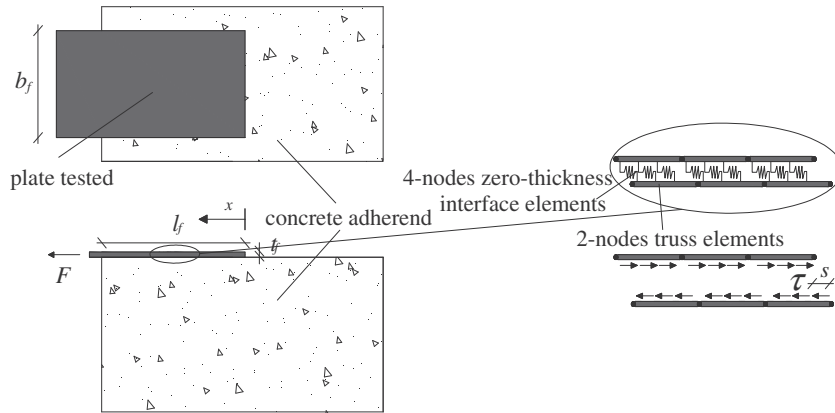


Fig. 1. FRP-to-concrete substrate pull-out scheme.

the joint to debond in shear fracture (under the hypothesis of pure mode II) due to an applied tangential stress  $\tau$ .

### 3.2. Thermal-dependent softening evolution

The evolution of the cracking surface is defined as function of the average temperature in the interface plane to take into account damage effects induced by thermal conditions. Particularly, the thermal damage is described through the  $\eta(\theta)$  of Eq. (7). A degradation rule describing this effect is proposed analogously to Eq. (8) and it is described as follows

$$\eta(\theta) = \frac{e^{-\zeta\theta}}{1 + (e^{-\zeta} - 1)\theta} \quad (10)$$

in which the  $\zeta$  parameter defines several possible decay curves of the thermal damage description (Fig. 2), while the  $\theta$  variable highlights the influence of the temperature through the following expression

$$\theta = \frac{1 - \cos\left(\pi \frac{T_{avg} - T_{avg,0}}{T_{avg,f} - T_{avg,0}}\right)}{2} \quad (11)$$

being  $T_{avg} = \frac{T^+ + T^-}{2}$  the average temperature in the interface plane, while  $T_{avg,0}$  and  $T_{avg,f}$  are two input temperatures. Particularly, if  $T_{avg} < T_{avg,0}$  (pull-out tests with low temperature) the interface is insensible to thermal effects, while  $T_{avg} > T_{avg,f}$  (tests under elevated temperature) means that the interface is totally debonded due to thermal processes.

In this work, the expressions (10) and (11) are also employed for defining the thermal damage parameter  $d_\tau$  controlling the thermal reduction of the elastic stiffness in Eq. (2)

$$d_\tau = 1 - \frac{e^{-\zeta_\tau\theta}}{1 + (e^{-\zeta_\tau} - 1)\theta} \quad (12)$$

being

$$\theta = \frac{1 - \cos\left(\pi \frac{T_{avg} - T_{avg,0}}{T_{avg,f} - T_{avg,0}}\right)}{2} \quad (13)$$

where  $\zeta_\tau$  defines several possible decay curves of the elastic stiffness decay against thermal processes.

### 3.3. Elasto-thermo-plastic constitutive rate equations

The classical elasto-thermo-plastic rate equations can be obtained by means of the consistency condition of Eq. (5)

$$\dot{f} = \frac{\partial f}{\partial \tau} \dot{\tau} + \frac{\partial f}{\partial \lambda} \dot{\lambda} + \frac{\partial f}{\partial T_{avg}} \dot{T}_{avg} = 0 \quad (14)$$

where the  $H$  softening parameter can be derived as follows

$$H = -\frac{\partial f}{\partial \lambda} = -\frac{\partial f}{\partial \tau_y} \frac{\partial \tau_y}{\partial w_{sl}} \frac{\partial w_{sl}}{\partial s^p} \frac{\partial s^p}{\partial \lambda} \quad (15)$$

in which  $\frac{\partial s^p}{\partial \lambda} = \frac{\partial f}{\partial \tau}$  as clearly highlighted in the plastic flow rule of Eq. (4).

Conversely, the temperature dependent softening parameter ( $I$ ) due to temperature effects can be defined as

$$I = -\frac{\partial f}{\partial T_{avg}} = -\frac{\partial f}{\partial \tau_y} \frac{\partial \tau_y}{\partial T_{avg}} \quad (16)$$

Then, the classical expression for the rate of the plastic multiplier is obtained by combining and solving Eq. (14), the constitutive Eq. (1) and Eqs. (15) and (16),

$$\dot{\lambda} = \frac{\frac{\partial f}{\partial \tau} k_{E,d} \left( \dot{s} - \alpha_s^0 \left[ \left| \Delta \dot{T} \right| \right] \right) - I \dot{T}_{avg}}{H + k_{E,d} \left( \frac{\partial f}{\partial \tau} \right)^2} \quad (17)$$

Consequently, the rate of the tangential interface stress is derived as function of the rate displacement and temperature jump as

$$\dot{\tau} = k_d^{ep} \dot{s} + \dot{\vartheta} \left( \dot{T} \right). \quad (18)$$

The tangential interface stiffness for elastic degradation expands into the same expression of the original model by Caggiano and Martinelli [41]

$$k_d^{ep} = k_{E,d} \left( 1 - \frac{\left( \frac{\partial f}{\partial \tau} \right)^2 k_{E,d}}{H + k_{E,d} \left( \frac{\partial f}{\partial \tau} \right)^2} \right) \quad (19)$$

while the rate of thermal tangential stress due to the rate of temperature jump is

$$\dot{\vartheta} \left( \dot{T}^+, \dot{T}^- \right) = k_{E,d} \left( \frac{\alpha_s^0 \left[ \left| \Delta \dot{T} \right| \right] \left( \frac{\partial f}{\partial \tau} \right)^2 + I \dot{T}_{avg} \frac{\partial f}{\partial \tau} - \alpha_s^0 \left[ \left| \Delta \dot{T} \right| \right]}{H + k_{E,d} \left( \frac{\partial f}{\partial \tau} \right)^2} \right). \quad (20)$$

The analytical expressions of the derivative terms needed in Eqs. (15) and (16) are reported in the following

$$\frac{\partial f}{\partial \tau} = 2 \tau, \quad (21)$$

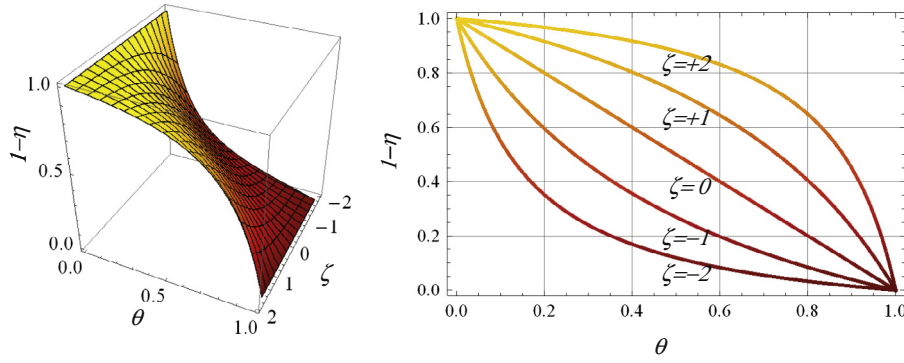


Fig. 2. Temperature-based law provided by Eq. (10): (a) tridimensional  $(1 - \eta, \theta, \zeta)$  and two-dimensional curves with fixed values for  $\zeta$ .

$$\frac{\partial f}{\partial \tau_y} = -2\tau_y, \quad (22)$$

$$\frac{\partial \tau_y}{\partial w_{sl}} = -\tau_{y,0}(1 - \eta) \frac{\partial \psi}{\partial \zeta} \frac{\partial \zeta}{\partial w_{sl}}, \quad (23)$$

$$\frac{\partial w_{sl}}{\partial s^p} = \tau, \quad (24)$$

$$\frac{\partial \tau_y}{\partial T_{avg}} = -\tau_{y,0}(1 - \psi) \frac{\partial \eta}{\partial \vartheta} \frac{\partial \vartheta}{\partial T_{avg}}. \quad (25)$$

#### 4. Interface heat transfer

The heat transfer throughout the FRP-to-concrete interface is governed by the following convective law

$$q_n = -h_f [|\Delta T|] \quad (26)$$

where  $h_f$  is the heat transfer coefficient while the discontinuity of the temperature field is defined as follows:

$$[|\Delta T|] = [T^+ - T^-] \neq 0. \quad (27)$$

The value of  $h_f$  mainly depends on the normal (“uplift”) and positive interface separation ( $u^+$ ) [39]: the following expression could be generally adopted for describing the  $h_f$ ,

$$h_f = h_f(u^+), \quad h_0 \geq h_f \geq h_{inf} \quad (28)$$

being  $h_0$  a maximum convective coefficient related to a closed crack ( $u^+ = 0$ ) while  $h_{inf}$  a minimum one which denotes the convective heat transfer for a fully opened crack.

However, since this paper deals with an interface formulation based on assuming a fracture process in pure “mode II” and, then, neglecting the effect of the interface normal (peeling) stresses (possibly resulting in out-of-plane displacements), the coefficient  $h_f$  can be taken as constant.

#### 5. Validation of the proposed model

Mechanical soundness and predictive capability of the model proposed in Section 3 need to be carefully assessed in a validation analysis which is presented in this section. Therefore, numerical analyses are performed to simulate the mechanical behaviour of pull-out tests on FRP strips glued on concrete substrates submitted to different temperatures.

First, the simulation of the temperature effect is simulated by considering a series of test results on double-lap shear tests as highlighted in Section 5.1. Then, the interdependence of thermal damage and mechanical softening is addressed in Section 5.2.

#### 5.1. Temperature effect on double-lap shear test

Experimental data focused on the effect of temperature on the double-lap shear test are available in the scientific literature [42] and are considered herein as a reference for the model validation. The numerical analyses are performed by taking into account of the proposed interface model into a User-defined interface constitutive law (UINTER) of Abaqus [43] implemented by the authors.

The experimental tests, performed by Klammer [42] and used in this work as a reference, deal with specimens heated in an oven during approximately 16 h and subsequently tested within 15 min. According to [42], all specimens, tested at elevated temperature, were packed with insulation during testing and the temperature of the concrete surface and the adhesive was measured with thermocouples. The temperature measurements oscillated within a range of 3 °C, meaning that a constant temperature can be considered for simulation purposes with a negligible error. The numerical examples refer to the main geometric and material properties described by the experimental evidences. Particularly, Table 1 highlights the material properties of the considered tests. The two component epoxy adhesive (Sikadur®-30) was used throughout the experimental research. The glass transition temperature of the Sikadur®-30 is approximately equal to 62 °C as given by the manufacturer [44].

The proposed interface model is employed to simulate the response of five specimens characterised by the same dimensions according to Fig. 1, with a bonding length  $l_f = 300$  mm, a plate width  $b_f = 50.0$  mm, a thickness  $t_f = 1.2$  mm and different temperatures ranging between the ambient temperature ( $T = 20$  °C) and the highest one ( $T = 90$  °C).

In this work, a constant value for the Young’s modulus of FRP,  $E_f = 165.0$  GPa, is assumed according to the test results exhibited in Klammer [42], however, a general temperature-based model which considers a  $E_f = E_f(T)$  relationship can be easily accounted in the FE problem. Moreover, the values of the relevant material parameters identified for the numerical simulation aimed at predicting the experimental tests, are the following: the shear stiffness  $k_E = 135.0$  MPa/mm, bond strength  $\tau_{y,0} = 5.50$  MPa, fracture energy of reference (at 20 °C)  $G_{f,20} = 0.62$  N/mm,  $\alpha = -1.0$ ,  $\alpha_s^0 = 2.5e-9$ , the convective heat transfer coefficient  $h_f = 1$  kW/m<sup>2</sup>/°C,  $T_{avg,0} = 20$  °C,  $T_{avg,f} = 130$  °C,  $\zeta = 0.0$ ,  $\zeta_\tau = 1.75$ . Finally, 100 interface elements are adopted in the FE model, with the aim of reducing discretisation errors.

The calibration procedure assumes that each specimen (tested at different temperatures) has different value of the fracture energy in mode II. Particularly, Fig. 3 reports the ratio between the calibrated fracture energy with that of reference at 20 °C against the considered temperature. It can be observed that once the glass transition temperature is reached or exceeded the

fracture energy value strongly decreases as the temperature increases. This aspect is confirmed in several works, among others to see [45,31,46,42]. Whereas, before the  $T_g$  limit, the fracture energy tends to increase against the temperature increment. This fact has not been well documented in literature and could derive from the natural randomness of the mechanical properties of the concrete substrate. The work of Wu et al. [45] actually reports a typical temperature-dependent reduction of the specific energy fracture, especially when  $T_g$  is reached or exceeded. As a matter of fact, above  $T_g$  temperature, the type of failure recorded in the experimental evidences changed from cracking in the concrete adjacent to the concrete-adhesive interface, leaving a small layer of concrete remaining attached to the adhesive, to failure exactly in between the concrete and the adhesive. This was accompanied by a significantly reduced scatter for the experimental force-slip curves [42].

Figs. 4–8 compare the results (in terms of applied force vs. slip at the loaded-end) obtained in the experimental tests for 20 °C, 40 °C, 50 °C, 70 °C and 90 °C with the corresponding numerical simulations obtained by assuming the proposed thermo-mechanical fracture-based discontinuous model for the softening branch. The agreement between experimental and numerical results is rather satisfactory, especially if it is kept in mind that the same sets of calibrated interface parameters were employed in all analyses.

Furthermore, the comparisons between the experimental results reported in Klamer [42] (dots) and the corresponding numerical simulations (continuous lines) in terms of strain distribution throughout the FRP strip length are shown in Fig. 9 for the test at ambient temperature (20 °C). Each curve corresponds to various load levels of the resulting relationship between the applied load and the maximum interface slip measured at the loaded end, represented in Fig. 4. The corresponding transferred shear interface stresses throughout the bonding length is reported in Fig. 10.

Moreover, the comparison of the numerical results against the experimental data can be directly proposed in terms of axial strains throughout the bonding length, under the various temperature levels for a considered load level of 30 kN (Figs. 4–7). Good agreement between numerical predictions and experimental results has been found for all tests as shown in Fig. 11. While the distribution of the shear interface stresses are shown in Fig. 12.

Figs. 4–11 demonstrate a rather good agreement between experimental results and numerical simulations based on the same set of input parameters needed by the proposed numerical model for describing both elastic and fracture responses combined with damage effects induced by thermal conditions of the FRP strip glued to a concrete substrate. Thus, the figures under consideration provide readers with a first demonstration of the soundness of the proposed fracture and temperature-based model.

5.2. Coupled thermomechanical debonding problem

As already mentioned in the introduction section, experimental works available in the scientific literature mainly described the thermal damage induced by elevated temperature in FRP bonded to concrete substrate under hot or residual conditions. However, the interdependence of thermal coupled with mechanical loads

Table 1 Model parameters according to the experimental tests by Klamer [42].

	Concrete	Adhesive	CFRP
Young's modulus ( $E_m$ ) [GPa]	31.1	12.8	165.0
Poisson's ratio ( $\nu$ )	0.20	0.30	0.35
Coeff. thermal exp. ( $\alpha$ ) 10E-6 [°C <sup>-1</sup> ]	11.30	26.00	-0.30

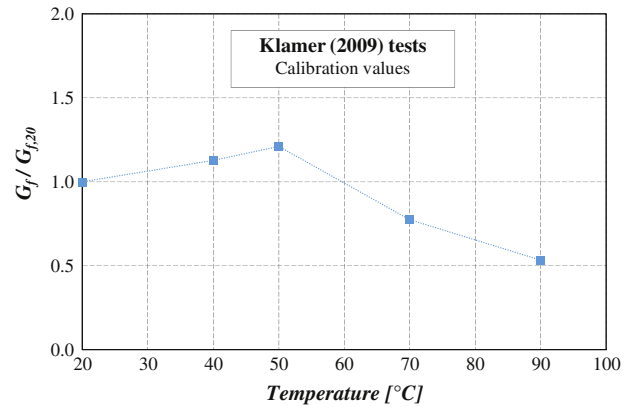


Fig. 3. Calibrated fracture energies vs. temperature.

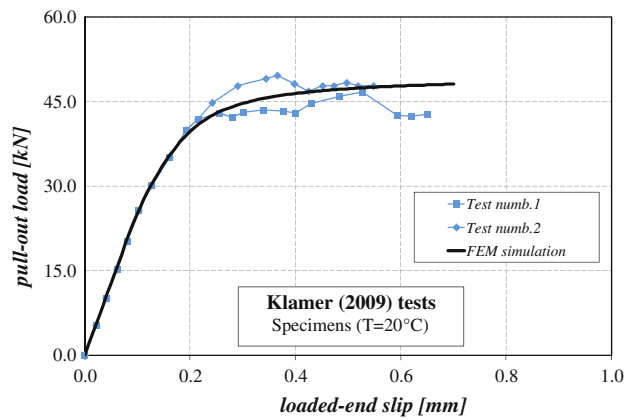


Fig. 4. Load-slip curve at the loaded-end: experimental results vs. FE-analyses for 20 °C.

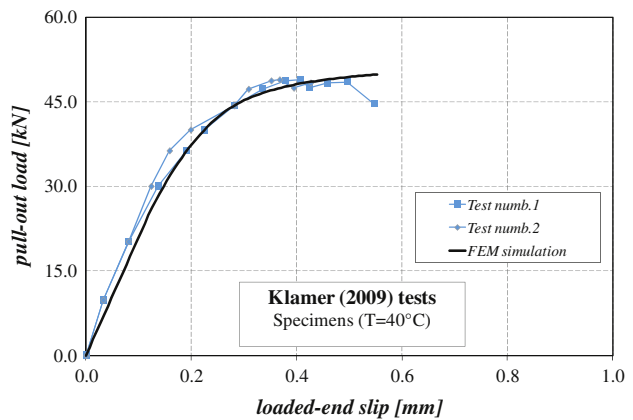


Fig. 5. Load-slip curve at the loaded-end: experimental results vs. FE-analyses for 40 °C.

represents a very important topic which needs to be addressed, especially when transient high temperature excursions are considered.

The double-lap shear test, analysed in the previous subsection, is now considered in order to study the coupled inter-dependence of temperature and mechanical loads. The same material parameters calibrated in the above subsections are used and four numerical examples are considered. The pull-out response in the four cases is governed by two load steps: (i) the first step in which an

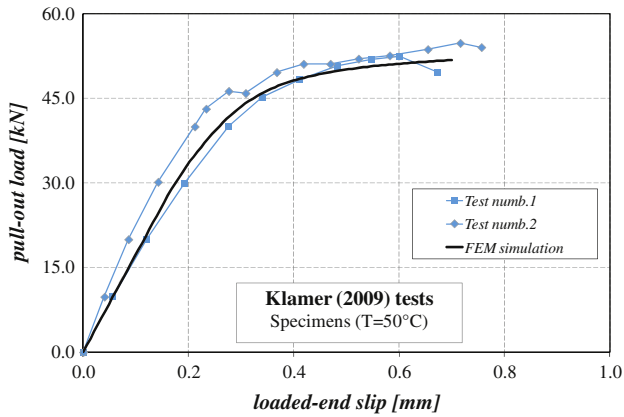


Fig. 6. Load-slip curve at the loaded-end: experimental results vs. FE-analyses for 50 °C.

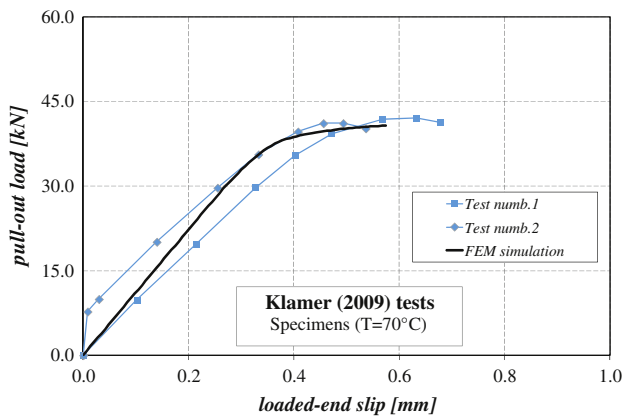


Fig. 7. Load-slip curve at the loaded-end: experimental results vs. FE-analyses for 70 °C.

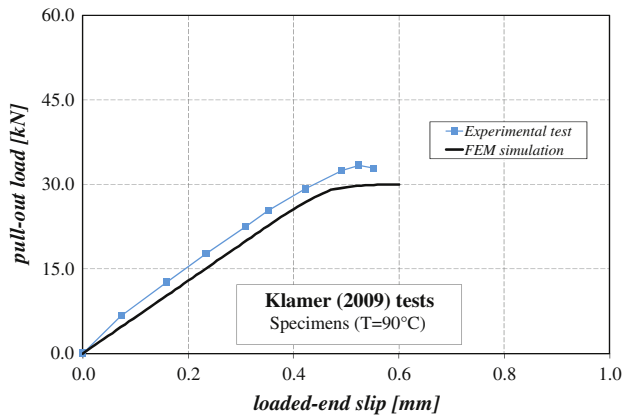


Fig. 8. Load-slip curve at the loaded-end: experimental results vs. FE-analyses for 90 °C.

applied total slip at 20 °C is imposed at loaded-end and (ii) in the second step a thermal-damage is produced through the imposition of a linear increment of the temperature (while the imposed slip at loaded-end was restrained to be constant). Fig. 13a reports the applied slip at loaded-end during the two time-steps while Fig. 13b deals with the temperature evolution during the time.

This analysis is aimed at exploring the effect of temperature of the mechanical response of the double-lap shear test adjusted in

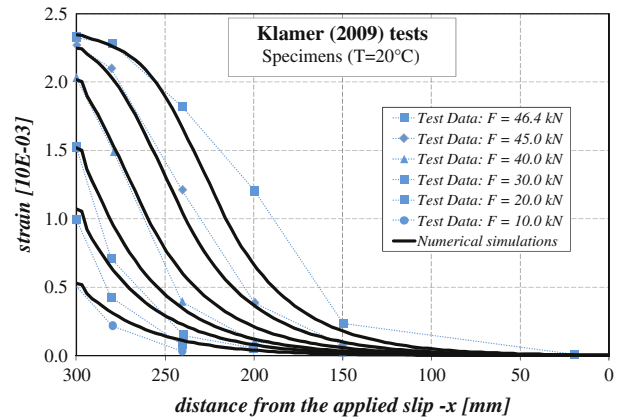


Fig. 9. Comparison in terms of axial strain distributions along the bonding length at ambient temperature and different load levels.

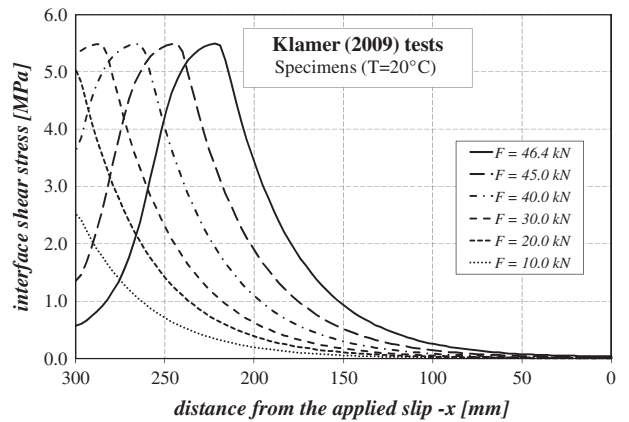


Fig. 10. Shear stress distributions along the bonding length at ambient temperature and different load levels.

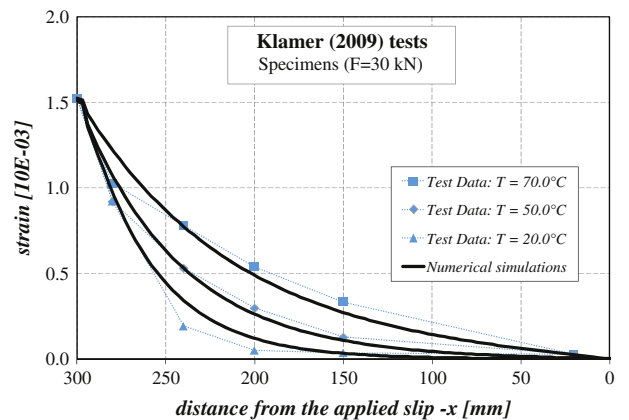


Fig. 11. Comparison in terms of axial strain distributions along the bonding length at a constant load of 30 kN and different temperatures.

Section 5.1. The numerical predictions allow for investigating the interaction of the thermal and mechanical degradation due to interface damage induced by thermal loads.

The main results of the coupled thermal/mechanical tests are shown in Fig. 14. At the top, Fig. 14a proposes the comparison between the load-slip curve obtained at ambient temperature and the four responses obtained when an increment of temperature is considered after a first time-step in which the applied slip

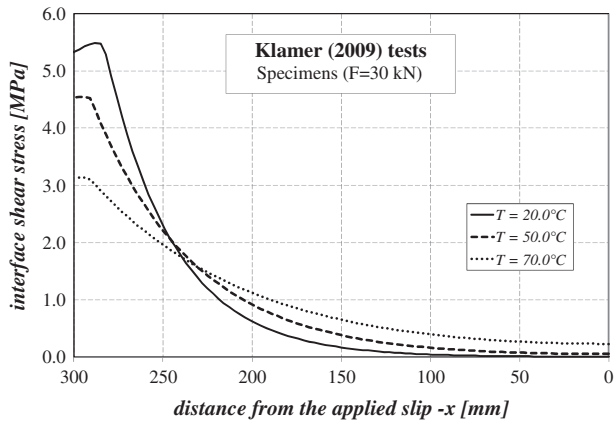


Fig. 12. Shear stress distributions along the bonding length at a constant load of 30 kN and different temperatures.

at loaded-end reaches a certain level. The four cases highlight that, for a fixed slip, a gradual increment of temperature leads to a gradual reduction of the pull-out load. Fig. 14b illustrates the pull-out load against the considered time-steps while Fig. 14c clearly reports the loss in pull-out strength due to an increment of the external temperature. The interface damage due to thermal effects leads to an overall release of the axial shear stresses and a subsequent loss of pull-out strength as represented in these figures.

6. Conclusions

A thermo-mechanical fracture-based solution for describing the overall bond behaviour of FRP-to-concrete interface submitted to high temperature was presented in this paper. A series of final remarks can be drawn out on the bases of both the model formulation and the proposed applications:

- Few theoretical models are currently available in the scientific literature for analysing the bond-slip behaviour of FRP-to-concrete interfaces at elevated temperature and all these models were mainly based on bond-slip relationships chosen “a priori”. The key parameters employed in such bond-slip models were principally determined from regression analysis of existing test data at elevated temperature while, this work provides readers with a more general formulation based on key fracture-mechanics principles combined with temperature effects inducing thermal damage.
- The detailed description of the incremental plasticity-based formulation of the model coupled with thermal damage were highlighted to the readers.

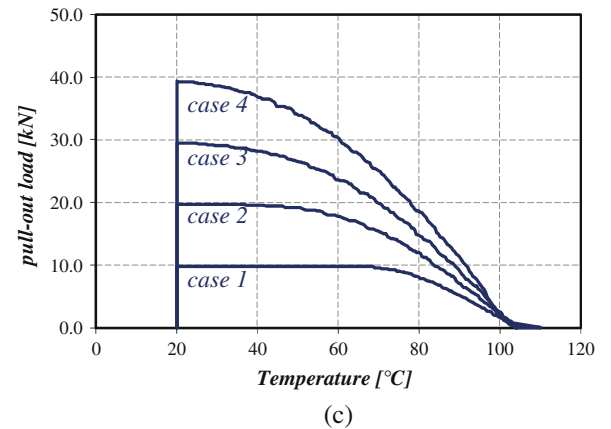
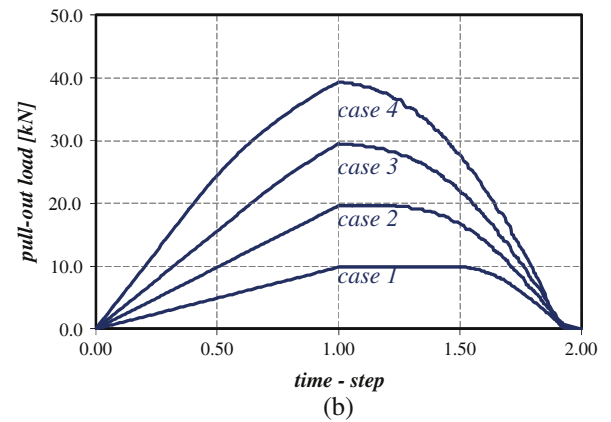
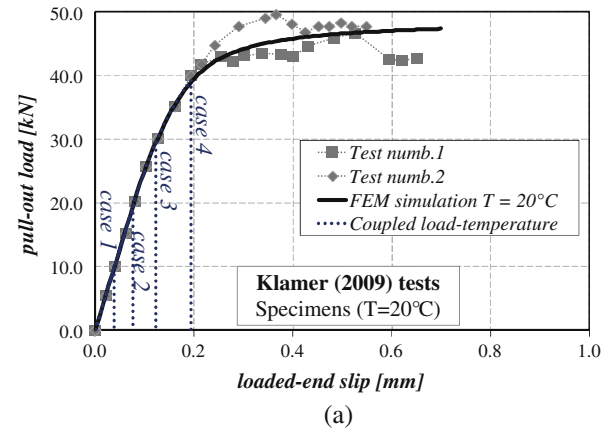


Fig. 14. Pull-out test under thermal coupled with mechanical loadings: (a) load-slip response, (b) load vs. time-step and (c) load vs. temperature.

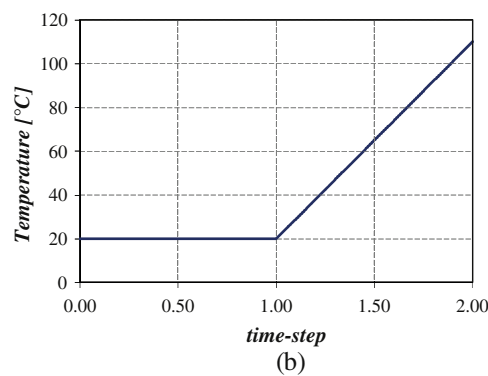
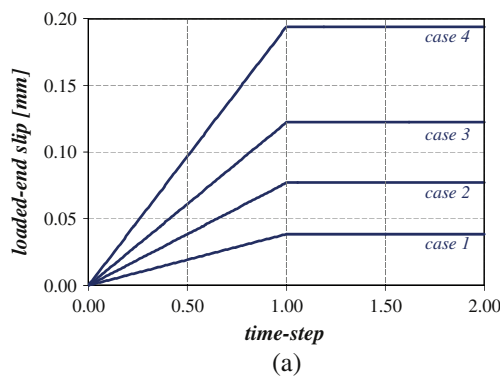


Fig. 13. Pull-out test under thermal coupled with mechanical loadings: (a) slip at the loaded-end and (b) temperatures history vs. time-step.

- Several numerical analyses were proposed by employing zero-thickness interface elements for simulating the results of some experimental tests reported in the scientific literature.
- Model performances demonstrate a rather good agreement between experimental results and numerical simulations based on the same set of input parameters needed by the proposed numerical model for describing both the fracture softening and thermal damage on the resulting response of the FRP laminate glued to a concrete substrate.
- The accuracy of the numerical simulation is achieved by just calibrating a temperature-based scaling function which thermally affects the strength and softening parameters defining the failure surface and the post-cracking response of the FRP-concrete joint.
- The extension of such comparisons to further experimental observations (especially in transient tests dealing with the interdependence of thermal and mechanical damage) is among the future steps of this research, which finally aims at characterising the force and displacement capacity of FRP-to-concrete joints subjected to high temperature.

### Acknowledgements

The support of INTI (Instituto Nacional de Tecnología Industrial, Argentina) and Roberto Rocca Education Program, through their respective grants, is gratefully acknowledged by the second author.

### References

- [1] Pepe M, Mazaheripour H, Barros J, Sena-Cruz J, Martinelli E. Numerical calibration of bond law for CFRP bars embedded in steel fibre-reinforced self-compacting concrete. *Compos Part B: Eng* 2013;50:403–12.
- [2] Martinelli E, Czaderski C, Motavalli M. Modeling in-plane and out-of-plane displacement fields in pull-off tests on FRP strips. *Eng Struct* 2011;33(12):3715–25.
- [3] Ghiassi B, Verstryngue E, Loureno PB, Oliveira DV. Characterization of debonding in FRP-strengthened masonry using the acoustic emission technique. *Eng Struct* 2014;66(0):24–34.
- [4] Ghiassi B, Marcarì G, Oliveira DV, Lourenco PB. Numerical analysis of bond behavior between masonry bricks and composite materials. *Eng Struct* 2012;43:210–20.
- [5] Barros JA, Dias SJ, Lima JL. Efficacy of CFRP-based techniques for the flexural and shear strengthening of concrete beams. *Cem Concr Compos* 2007;29(3):203–17.
- [6] Michels J, Sena-Cruz J, Czaderski C, Motavalli M. Structural strengthening with prestressed CFRP strips with gradient anchorage. *J Compos Constr* 2013;17(5):651–61.
- [7] Jia J, Davalos JF. Loading variable effects on mode-I fatigue of wood-FRP composite bonded interface. *Compos Sci Technol* 2004;64(1):99–107.
- [8] Realfonzo R, Martinelli E, Napoli A, Nunziata B. Experimental investigation of the mechanical connection between FRP laminates and concrete. *Compos Part B: Eng* 2013;45(1):341–55.
- [9] Teng J, Chen JF, Smith ST, Lam L. FRP: strengthened RC structures, vol. 1. Wiley-VCH; 2002.
- [10] Bilotta A, Ludovico MD, Nigro E. FRP-to-concrete interface debonding: experimental calibration of a capacity model. *Compos Part B: Eng* 2011;42(6):1539–53.
- [11] Bilotta A, Faella C, Martinelli E, Nigro E. Design by testing procedure for intermediate debonding in EBR FRP strengthened RC beams. *Eng Struct* 2013;46(0):147–54.
- [12] Lu X, Teng J, Ye L, Jiang J. Bondslip models for FRP sheets/plates bonded to concrete. *Eng Struct* 2005;27(6):920–37.
- [13] Baky HA, Ebead U, Neale K. Nonlinear micromechanics-based bondslip model for FRP-concrete interfaces. *Eng Struct* 2012;39(0):11–23.
- [14] Yu B, Till V, Thomas K. Modeling of thermo-physical properties for FRP composites under elevated and high temperature. *Compos Sci Technol* 2007;67(1516):3098–109.
- [15] Czaderski C, Martinelli E, Michels J, Motavalli M. Effect of curing conditions on strength development in an epoxy resin for structural strengthening. *Compos Part B: Eng* 2012;43(2):398–410.
- [16] Bai Y, Keller T, Valle T. Modeling of stiffness of FRP composites under elevated and high temperatures. *Compos Sci Technol* 2008;68(1516):3099–106.
- [17] Foster S, Bisby L. Fire survivability of externally bonded FRP strengthening systems. *J Compos Constr* 2008;12(5):553–61.
- [18] Biscaia HC, Chastre C, Viegas A, Franco N. Numerical modelling of the effects of elevated service temperatures on the debonding process of FRP-to-concrete bonded joints. *Compos Part B: Eng* 2014, ISSN 1359-8368. <http://dx.doi.org/10.1016/j.composites.b.2014.10.041>.
- [19] Chowdhury E, Eedson R, Bisby L, Green M, Benichou N, Kodur, et al. Mechanical characterization of fibre reinforced polymers for numerical fire endurance modelling. In: *Proceeding of the fifth international conference-structures in fire*; 2008. p. 28–30.
- [20] Chowdhury E, Eedson R, Bisby L, Green M, Benichou N. Mechanical characterization of fibre reinforced polymers materials at high temperature. *Fire Technol* 2011;47(4):1063–80.
- [21] Kumahara S, Masuda Y, Tanano H, Shimizu A. Tensile strength of continuous fiber bar under high temperature, vol. 138. *ACI Special Publication*; 1993.
- [22] Wang Y, Wong P, Kodur V. An experimental study of the mechanical properties of fibre reinforced polymer (FRP) and steel reinforcing bars at elevated temperatures. *Compos Struct* 2007;80(1):131–40.
- [23] Bisby L. Fire behavior of fiber-reinforced polymer (FRP) reinforced or confined concrete. Ph.D. thesis. Kingston (Ontario, Canada): Queens Univ.; 2003.
- [24] Dai JG, Gao W, Teng J. Bond-slip model for FRP laminates externally bonded to concrete at elevated temperature. *J Compos Constr* 2012;17(2):217–28.
- [25] Borchert K, Zilch K. Time depending thermo mechanical bond behavior of epoxy bonded pre-stressed FRP-reinforcement. In: *Proceedings of the 7th international symposium on fiber reinforced polymer (FRP) reinforcement for concrete structures (FRPRCS7)*; 2005. p. 671–84.
- [26] Bootle J, Burzesi F, Fiorini L. Design guidelines. *ASM handbook, composites, vol. 21. Material Park (Ohio): ASM International*; 2001. p. 388–95.
- [27] ACI440-2R-08. Guide for the design and construction of externally bonded FRP systems for strengthening concrete structures. Farmington Hills (MI): American Concrete Institute; 2008.
- [28] Tadeu AJ, Branco FJ. Shear tests of steel plates epoxy-bonded to concrete under temperature. *J Mater Civ Eng* 2000;12(1):74–80.
- [29] Blontrock H, Taerwe L, Vanwalleghem H. Bond testing of externally glued FRP laminates at elevated temperature. In: *Proceeding of the international conference bond in concrete-from research to standard, Budapest, Hungary*; 2002. p. 64854.
- [30] Klammer EL, Hordijk DA, Janssen HJ. The influence of temperature on the debonding of externally bonded CFRP. In: *Proc, 7th int symp on fiber reinforcement polymer reinforcement for concrete structures (FRPRCS-7)*; 2005. p. 1551–70.
- [31] Wu Z, Iwashita K, Yagashiro S, Ishikawa T, Hamaguchi Y. Temperature effect on bonding and debonding behavior between FRP sheets and concrete. *J Soc Mater Sci* 2005;54(5):474–80.
- [32] Leone M, Matthys S, Aiello MA. Effect of elevated service temperature on bond between FRP EBR systems and concrete. *Compos Part B: Eng* 2009;40(1):85–93.
- [33] Di Tommaso A, Neubauer U, Pantuso A, Rostasy F. Behavior of adhesively bonded concrete-CFRP joints at low and high temperatures. *Mech Compos Mater* 2001;37(4):327–38.
- [34] CNR-DT200/2006. Guide for the design and construction of externally bonded FRP systems for strengthening existing structures. Materials, RC and PC structures, masonry structures. National Research Council, Rome-CNR; 2006.
- [35] fib Bulletin-No.14. Externally bonded FRP reinforcement for RC structures. Technical report. fib- The International Federation for Structural Concrete; 2001.
- [36] Cornetti P, Carpinteri A. Modelling the FRP-concrete delamination by means of an exponential softening law. *Eng Struct* 2011;33:1988–2001.
- [37] Ferracuti B, Savoia M, Mazzotti C. A numerical model for FRP-concrete delamination. *Compos Part B: Eng* 2006;37:356–64.
- [38] Gamage J, Al-Mahaidi R, Wong M. Bond characteristics of CFRP plated concrete members under elevated temperatures. *Compos Struct* 2006;75(1–4):199–205.
- [39] Willam K, Rhee I, Shing B. Interface damage model for thermomechanical degradation of heterogeneous materials. *Comput Methods Appl Mech Eng* 2004;193(30–32):3327–50.
- [40] Carol I, Prat P, Lopez C. Normal/shear cracking model: applications to discrete crack analysis. *J Eng Mech – ASCE* 1997;123:765–73.
- [41] Caggiano A, Martinelli E. A fracture-based interface model for simulating the bond behaviour of FRP strips glued to a brittle substrate. *Compos Struct* 2013;99(0):397–403.
- [42] Klammer EL. Influence of temperature on concrete beams strengthened in flexure with CFRP. Eindhoven, the Netherlands: PhD Thesis. Eindhoven: Technische Universiteit; 2009.
- [43] ABAQUS. ABAQUS documentation. Dassault systems, Providence, RI, USA; 2012.
- [44] Sika. Sikadur 30. Sika Group; 2009. <[www.sika.com](http://www.sika.com)>.
- [45] Wu Z, Iwashita K, Yagashiro S, Isshikawa T, Hamaguchi Y. Temperature effect on bonding and debonding behavior between FRP sheets and concrete. In: *Proceedings of FRP composites in civil engineering – CICE 2004, Adelaide (Australia)*; 2004. p. 905–12.
- [46] Nigro E, Manfredi G, Cosenza E, Zappoli M. Effects of high temperature on the performances of RC bridge decks strengthened with externally bonded FRP reinforcement. In: *Federation internationale du Beton. Proceedings of the 2nd international congress. Naples: fib*; 2006.